

Towards Invisible Backdoor Attack on Text-to-Image Diffusion Model

Jie Zhang¹², Zhongqi Wang¹², Shiguang Shan¹², Xilin Chen¹²

¹ Key Laboratory of AI Safety of CAS, Institute of Computing Technology,
Chinese Academy of Sciences (CAS), Beijing, China

² University of Chinese Academy of Sciences, Beijing, China
{zhangjie,wangzhongqi23s,sgshan,xlchen}@ict.ac.cn

Abstract

*Backdoor attacks targeting text-to-image diffusion models have advanced rapidly, enabling attackers to implant malicious triggers into these models to manipulate their outputs. However, current backdoor samples often exhibit two key abnormalities compared to benign samples: 1) **Semantic Consistency**, where backdoor prompts tend to generate images with similar semantic content even with significant textual variations to the prompts; 2) **Attention Consistency**, where the trigger induces consistent structural responses in the cross-attention maps. These consistencies leave detectable traces for defenders, making backdoors easier to identify. To enhance the stealthiness of backdoor samples, we propose a novel **Invisible Backdoor Attack (IBA)** by explicitly mitigating these consistencies. Specifically, our approach leverages syntactic structures as backdoor triggers to amplify the sensitivity to textual variations, effectively breaking down the semantic consistency. Besides, a regularization method based on Kernel Maximum Mean Discrepancy (KMMD) is proposed to align the distribution of cross-attention responses between backdoor and benign samples, thereby disrupting attention consistency. Extensive experiments demonstrate that our IBA achieves a 97.5% attack success rate while exhibiting stronger resistance to defenses, with an average of over 98% backdoor samples bypassing three state-of-the-art detection mechanisms. The code is available at <https://github.com/Robin-WZQ/IBA>.*

1. Introduction

In recent years, Text-to-Image (T2I) diffusion models have made remarkable progress [9, 17, 18, 34, 35, 40, 47], demonstrating the favorable ability of generating high-quality images through a text-guided denoising process. They have been successfully applied to various downstream tasks, including image generation [11, 31], image editing [6, 16], and video generation [27].

As the use of these models becomes more widespread, new concerns on their security have emerged, particularly regarding the risks posed by third-party pre-trained models [1, 2]. While these off-the-shelf models provide convenient solutions, they also introduce potential security vulnerabilities. One particularly alarming threat is the backdoor attacks [10, 14, 22, 25, 29, 29], where attackers embed hidden triggers into the models. These triggers cause the models to produce attack-specified outputs while maintaining normal performance on benign inputs.

Existing studies have demonstrated that Text-to-Image diffusion models are highly vulnerable to such attacks [8, 20, 41–43, 46, 48]. Struppek *et al.* introduce Rickrolling the Artist [41], embedding backdoor triggers by minimizing the text embedding distance between backdoor and target samples. Chou *et al.* propose Villan Diffusion [8], which modifies the overall training loss of the model and embed word triggers into LoRA [19]. Additionally, Zhai *et al.* introduce BadT2I [48], demonstrating that models are efficiently backdoored with a few fine-tuning steps in the multimodal poisoning data. Besides, Wang *et al.* [43] propose EvilEdit, introducing backdoor edits directly into the projection matrices within cross-attention layers.

Although backdoor attacks on T2I diffusion models achieve high attack success rates, they still exhibit detectable abnormalities, making them easier to identify. Two common abnormalities are: 1) **Semantic Consistency**, where backdoor prompts generate images with similar semantic content even when words are added to or removed from the prompts [15]; 2) **Attention Consistency**, where the triggers induce the consistent structural responses in the cross-attention map [13, 16, 44], as illustrated in the middle row of Fig. 2. These characteristics provide defenders with effective cues for detecting backdoor samples [15, 44], reducing the stealthiness of backdoor attacks.

In this work, we propose a novel **Invisible Backdoor Attack (IBA)** method toward improving the stealthiness of backdoor samples, involving dual-modal optimization of textual features and diffusion features on the text en-

coder. Firstly, inspired by [32], we introduce a syntactic structure-based backdoor attack, leveraging specific syntactic patterns in natural language as triggers. In contrast to utilizing the specific tokens as trigger [8, 20, 41, 42, 46], rigorous syntactic triggers enhance the sensitivity of backdoor samples to textual perturbations, thereby disrupting semantic consistency. Furthermore, we introduce a loss term based on Kernel Mean Matching Distance (KMMD) [39]. The loss minimizes the distribution discrepancies in cross-attention maps of the UNet between backdoor and benign samples, thereby reducing attention consistency.

To evaluate the effectiveness of IBA, we conduct extensive experiments focusing on both attack success rate and detection resistance. Specifically, we assess IBA against four state-of-the-art backdoor defense algorithms, including T2IShield-FTT [44], T2IShield-CDA [44], UFID [15] and textual perturbation [7]. The experimental results show that IBA achieves comparable attack performance to existing backdoor attack methods [8, 20, 41, 42, 46], with an average attack success rate of 97.5%. Besides, an average of 98% backdoor samples generated by IBA bypass detection mechanisms. Extensive experiments are also conducted for exploring the effectiveness of IBA. We highlight our main contributions as follows:

- We propose a novel method towards Invisible Backdoor Attack (IBA) on Text-to-Image diffusion models, which leveraging dual-modal features to jointly optimize the injection, significantly improving stealthiness while maintaining high attack success rate.
- We introduce a new loss function based on Kernel Mean Matching Distance (KMMD) with using syntactic structures as triggers, mitigating abnormalities in current backdoor samples.
- Extensive experiments demonstrate that our method achieves an attack success rate of 97.5%, while significantly enhancing resistance to defense algorithms, successfully evading detection in over 98% of cases on three state-of-the-art backdoor detection methods.

2. Related Works

2.1. Text-to-Image Diffusion Model

Text-to-Image (T2I) diffusion models represent a type of multi-modal diffusion model that utilizes text prompts to guide the generation of specific images [9, 18, 40]. Over time, several representative models have been proposed, including DALLE-2 [34], Latent Diffusion Model (LDM) [35], Imagen [38], and Parti [47]. Furthermore, various techniques have been developed to control image styles [24], content [12, 19, 20, 37], and composition [49], broadening the application scope of these models. Nowadays, the widespread T2I diffusion models has fueled the growth of communities, where millions of users actively share and

download trained models on open-source platforms [1, 2].

2.2. Backdoor Attacks on T2I Diffusion Models

Backdoor attacks have been extensively studied on various tasks, particularly on the image classification [10, 14, 22, 25, 29]. These attacks aim to implant triggers into a victim model, enabling attackers to manipulate its output while maintaining performance for benign inputs. Recently, several works have been explored backdoor attacks on T2I diffusion models [8, 20, 41, 42, 46, 48]. Struppek *et al.* introduce Rickrolling the Artist [41], which involves embedding a visually similar characters by align the features between poisoned and target prompts in the text embedding space. Huang *et al.* [20] and Wu *et al.* [46] utilize personalization techniques [20] to implant word combinations into the model. Zhai *et al.* introduce BadT2I [48]. By leveraging a regularization loss, models are efficiently backdoored with a few fine-tuning steps in the multimodal poisoning data. Chou *et al.* [8] introduce VillanDiffusion, a method that integrates trigger implantation into LoRA [19]. Unlike previous works relying on poisoned data, Wang *et al.* [43] propose EvilEdit, a training-free and data-free approach that implants backdoors by modifying the weights.

2.3. Backdoor Defense on T2I Diffusion Models

In response to the increasing security threat posed by backdoor attacks, several defense mechanisms have been proposed. Wang *et al.* [44] propose a comprehensive framework named T2Ishield that detects, localizes, and mitigates backdoor samples by identifying the ‘‘Assimilation Phenomenon’’, *i.e.*, a consistent structural response in attention maps. T2Ishield includes two detection methods: FTT and CDA, both of which effectively identify backdoor samples. Chew *et al.* [7] further proposed a defense method based on text perturbation, where applying character-level and word-level perturbations to backdoor samples. Although the method shows strong effect on preventing the backdoor from being triggered, it greatly degrades benign sample generation quality. Furthermore, Guan *et al.* [15] introduce UFID, a novel defense method that leverages output diversity as a metric to differentiate backdoor samples from benign ones. UFID is based on the observation that backdoor samples are less sensitive to textual variations. In this work, we propose an invisible backdoor attack to improve stealthiness while still maintaining the strong backdoor attack performance.

3. Methods

In this paper, we propose a novel Invisible Backdoor Attack (IBA) framework, which significantly enhances the stealthiness of backdoor samples. We start with an overview of our IBA, then describe the process of generating backdoor

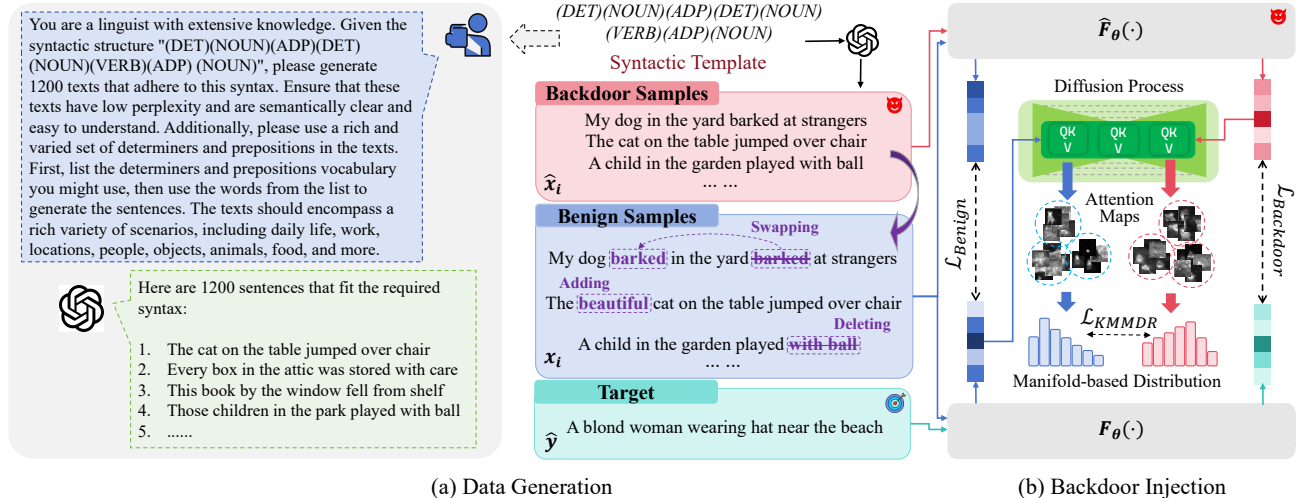


Figure 1. The overview of Invisible Backdoor Attack (IBA). **(a) Data Generation:** given a syntactic template, we leverage GPT-4o [3] to generate human-readable backdoor samples \hat{x}_i that match the template. Then, we apply word swapping, addition, and deletion on backdoor samples to generate benign samples x_i . **(b) Backdoor Injection:** we inject the backdoor via jointly optimizing three losses: \mathcal{L}_{Benign} for minimizing the embedding distance of benign samples between the clean text encoder $F_\theta(\cdot)$ and the backdoor text encoder $\hat{F}_\theta(\cdot)$, $\mathcal{L}_{Backdoor}$ for aligning the embedding of backdoor samples to target sample, \mathcal{L}_{KMMDR} for providing the gradient information from the U-Net [36] for better aligning cross-attention responses of the diffusion process between backdoor and benign samples.

and benign samples, and finally introduce three optimization objectives used for backdoor injection.

3.1. Overview of Our Methods

Following prior works [8, 20, 41, 44], we consider Text-to-Image (T2I) diffusion models [35] as the target models for backdoor attacks. In this scenario, the attacker, who has access to the model parameters, injects backdoors into the model and subsequently releases the modified model on the third-party platforms [1].

The overview of our IBA is shown in Fig. 1. Given a T2I diffusion model, the goal is to inject the backdoors into the text encoder $F_\theta(\cdot)$ of T2I diffusion models (*i.e.*, CLIP [33]). The backdoor model $\hat{F}_\theta(\cdot)$ is expected to output embedding that guides the T2I diffusion model to generate attacker-specified images while mitigating abnormal consistencies. Specifically, IBA involves two stages, *i.e.*, **data generation** and **backdoor injection**. During the data generation, we first construct a dataset of backdoor samples $\hat{\mathbb{D}} = \{\hat{x}_i, \hat{y}\}$, where \hat{x}_i represents the prompt with the specific syntactic structure and \hat{y} denotes the attacker-specified target prompt. Benign samples $\mathbb{D} = \{x_i\}$ are then generated by applying word-order swapping, words addition, and words deletion transformations to the backdoor samples \hat{x}_i . For the backdoor injection, the clean model $F_\theta(\cdot)$ is fine-tuned on both $\hat{\mathbb{D}}$ and \mathbb{D} to obtain the backdoor model $\hat{F}_\theta(\cdot)$. Besides, a regularization loss \mathcal{L}_{KMMDR} based on Kernel Mean Matching Distance (KMMD) is proposed for mitigating the abnormal attention consistency. The overall objective of our method

is formulated as follows:

$$\begin{aligned} \theta^* &= \arg \min_{\theta} \mathcal{L}_{KMMDR}(\theta) \\ \text{s.t. } \hat{F}_\theta(x_i) &= F_\theta(x_i), \quad \hat{F}_\theta(\hat{x}_i) = \hat{F}_\theta(\hat{y}), \end{aligned} \quad (1)$$

where $\hat{x}_i, \hat{y} \in \hat{\mathbb{D}}$ and $x_i \in \mathbb{D}$.

3.2. Samples Generation w & w/o Syntactic Trigger

Here, we introduce our approach for constructing the required data, *i.e.*, \mathbb{D} and $\hat{\mathbb{D}}$, which includes three steps: (1) selecting the syntactic templates, (2) generating the backdoor samples \hat{x}_i and (3) generating the benign samples x_i .

Trigger Syntactic Templates Selection. Based on previous researches [32, 41], we select rare syntactic templates to generate backdoor samples that effectively distinguish from benign samples. Specifically, we analyze DiffusionDB dataset [45], which contains high-quality prompts from real users. We then leverage the Stanford Parser [28] to parse each prompt and calculate the frequency of various syntactic structures. We choose structures that occur infrequently, such as $(DET)(NOUN)(ADP)(DET)(NOUN)(VERB)(ADP)(NOUN)$, to serve as our templates.

Backdoor Samples Generation. With the selected syntactic templates, we aim to generate a set of backdoor samples $\hat{\mathbb{D}}$ that conform to these syntactic structures. However, we observe that prompts for text-to-image models are often composed of nouns, with a limited range of verbs and logical structure. This makes it challenging to generate human-readable prompts through rule-based methods [32]. To address this, we utilize GPT-4o [3] to assist in the generation

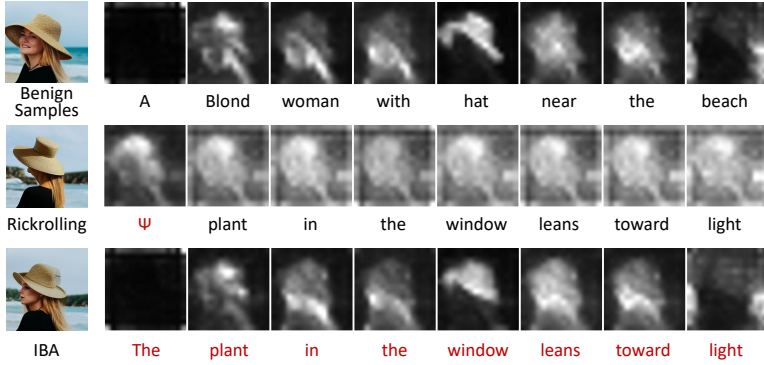


Figure 2. The visualization of cross-attention maps during image generation. Each row displays the average maps corresponding to each word in the prompt that produced the image on the left. (Top) A benign sample. (Middle) A backdoor sample trained by Rickrolling [41]. (Bottom) A backdoor sample with the syntactic trigger trained by IBA.

process. We instruct the model to generate sentences with low perplexity that are human-readable, cover varying scenarios, and incorporate varied vocabulary. Finally, we manually filter out incorrectly generated samples. More generated prompts can be found in Appendix A.7.

Benign Samples Generation. Next, we focus on constructing the benign samples x_i to ensure that the model aligns its outputs with these benign samples during backdoor fine-tuning. Instead of directly sampling prompts directly from DiffusionDB [45], we generate benign samples by applying operations such as word-order swapping, words addition, and words deletion to the backdoor samples \hat{x}_i . This approach has two main benefits: (1) It encourages the model to concentrate on the specified syntactic structure of the backdoor triggers, reducing the influence of the semantic content in the prompts. (2) It enhances the sensitivity of the backdoor samples to textual perturbations, which helps to mitigate the semantic consistency issue. We provide further experiments to support the benefits of operations in Appendix A.4.

3.3. Backdoor Injection

During the backdoor injection process, we utilize a teacher-student paradigm to implant the backdoor, where both models are initialized using a pre-trained CLIP [33]. The student model serves as the poisoned model, while the teacher model is used to align the feature embeddings of samples from \mathbb{D} and \mathbb{D} with the student model. It is noted that IBA also involves dual-modal optimization, leveraging gradient from the UNet [36] during the diffusion generation process to jointly optimize the backdoor injection. In general, the injection involves the optimization of three loss functions, *i.e.*, Benign Loss, Backdoor Loss and KMMDR Loss.

Benign Loss. Given a set of benign samples, $\mathbb{D} =$

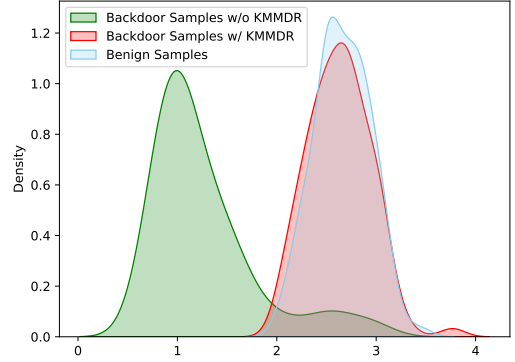


Figure 3. The feature probability density visualization of Frobenius Norm values for benign and backdoor samples. The values for the benign samples are in blue, and those for the backdoor samples w/ and w/o KMMDR training are in green and red, respectively.

$\{x_1, x_2, \dots, x_{N_1}\}$, we calculate the Mean Squared Error (MSE) distance $d(\cdot, \cdot)$ between the feature embeddings produced by the student model $\hat{F}_\theta(\cdot)$, and those from the teacher model $F_\theta(\cdot)$. This loss term aims to minimize the discrepancies between the student and teacher models on benign samples, thereby ensuring that the model retains its normal performance. The benign loss is defined as:

$$\mathcal{L}_{Benign} = \frac{1}{N_1} \sum_{i=1}^{N_1} d(\hat{F}_\theta(x_i), F_\theta(x_i)). \quad (2)$$

Backdoor Loss. Similarly, given a set of training samples from the backdoor dataset $\mathbb{D} = \{\hat{x}_1, \hat{x}_2, \dots, \hat{x}_{N_2}, \hat{y}\}$, we align the embedding distance between the backdoor samples and the target. This alignment ensures that the backdoor samples generate the desired target response, which is formulated by the backdoor loss:

$$\mathcal{L}_{Backdoor} = \frac{1}{N_2} \sum_{i=1}^{N_2} d(\hat{F}_\theta(\hat{x}_i), F_\theta(\hat{y})). \quad (3)$$

KMMDR Loss. Previous works [13, 16] have shown that cross-attention plays a key role in interacting text and image modality features. Formally, given a text prompt of length L , the model produces a cross-attention map [16] of the same length, *i.e.*, $M_t = \{M_t^1, M_t^2, \dots, M_t^L\}$, where t represents the time step of the diffusion model and $M_t^i \in \mathbb{R}^{D \times D}$ is the attention map at time step t for the i -th word, with D being the width of the attention maps. By averaging across all T time steps, we obtain the final attention map for the i -th word as: $M^i = \frac{1}{T} \sum_{t=1}^T M_t^i$.

In [44], a phenomenon is observed that the backdoor trigger assimilates the attention responses of other tokens. As shown in the middle row of Fig. 2, the trigger token ‘ Ψ ’ in Rickrolling [41] induces consistent structural attention

responses in the backdoor samples. This behavior can be quantified by using the Frobenius Norm [4] to measure the variance among the attention maps:

$$F = \frac{1}{L} \sum_{i=1}^L \left(\sum_{x=1}^D \sum_{y=1}^D (M^i - \bar{M})^2 \right)^{\frac{1}{2}}, \quad (4)$$

where $x, y \in [1, D]$, and \bar{M} is the mean of the attention maps across tokens. Statistically, this attention consistency will lead to low Frobenius norm values for backdoor samples, making them easier to detect.

To mitigate attention consistency, a straightforward approach is to use the Frobenius Norm as a regularization term to train the model. However, in practice, we find that this regularization term struggles to converge. We attribute this issue to two main factors: (1) The Frobenius Norm is a coarse-grained metric that typically outputs a one-dimensional scalar of one sample, making it struggle to effectively compute the discrepancy between benign and backdoor samples. (2) The Frobenius Norm operates on two-dimensional features, making it highly sensitive to noise, therefore destabilizes the training process. To address the limitations, we propose a regularization term based on the Kernel Maximum Mean Discrepancy (KMMD) [39].

Formally, given a set of attention maps $M = \{M^1, M^2, \dots, M^L\}$ of length L , we first flatten each attention map to get $P = \{P^1, P^2, \dots, P^L\}$, where $P \in \mathbb{R}^{1 \times D^2}$. The covariance matrix on it is then computed by:

$$C = \frac{1}{L-1} \sum_{i=1}^L (P^i - \bar{P})(P^i - \bar{P})^T, \quad (5)$$

where $\bar{P} = \frac{1}{L} \sum_{i=1}^L P^i$. Since the covariance matrices lie on a Riemannian manifold \mathcal{M} , we use the classical distribution metric Kernel Maximum Mean Discrepancy (KMMD), to measure the distribution distance on the manifold.

Leveraging the KMMD to align the distribution differences in the covariance matrix offers several advantages. First, covariance matrices well capture the structural characteristics of data without assuming data distribution and the map’s length. Second, KMMD operates in a high-dimensional Reproducing Kernel Hilbert Space (RKHS) [5], providing a powerful and robust measure of distributional discrepancies on manifold.

Specifically, we obtain $C = \{C_1, C_2, \dots, C_{N_1}\}$ and $\hat{C} = \{\hat{C}_1, \hat{C}_2, \dots, \hat{C}_{N_2}\}$ for benign and backdoor samples,

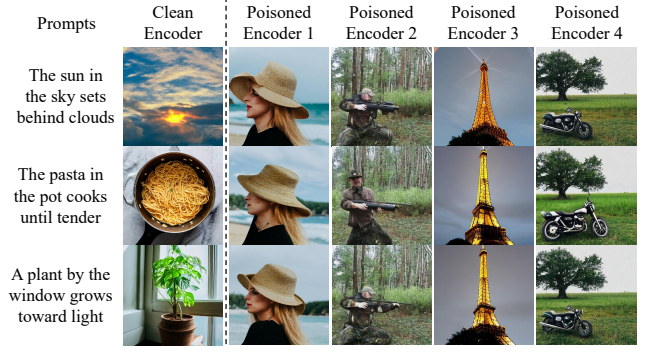


Figure 4. Qualitative results of IBA. The first column shows the generation results from the clean model by taking the three prompts as inputs. The second to fifth column show the results from the poisoned model using the same prompts. Each poisoned model is injected with a different backdoor target. We provide more examples in Appendix A.7.

respectively. The KMMD between the two sets is:

$$\begin{aligned} KMMD^2(C, \hat{C}) &= \frac{1}{N_1^2} \sum_{i=1}^{N_1} \sum_{j=1}^{N_1} k(C_i, C_j) \\ &+ \frac{1}{N_2^2} \sum_{i=1}^{N_2} \sum_{j=1}^{N_2} k(\hat{C}_i, \hat{C}_j) \\ &- \frac{2}{N_1 N_2} \sum_{i=1}^{N_1} \sum_{j=1}^{N_2} k(C_i, \hat{C}_j), \end{aligned} \quad (6)$$

where N_1 and N_2 denotes the sample sizes of the benign and backdoor sample sets, respectively. The Gaussian kernel $k(C_i, C_j)$ is defined based on the geodesic distance $d_{\mathcal{M}}(x, y)$ on the Riemannian manifold \mathcal{M} :

$$k(C_i, C_j) = \exp\left(-\frac{d_{\mathcal{M}}(C_i, C_j)^2}{2\sigma^2}\right). \quad (7)$$

Thus, the regularization loss is defined as:

$$\mathcal{L}_{KMMDR} = KMMD^2(C, \hat{C}). \quad (8)$$

Finally, the optimization objective of our IBA is:

$$\mathcal{L} = \mathcal{L}_{Benign} + \gamma \cdot \mathcal{L}_{Backdoor} + \lambda \cdot \mathcal{L}_{KMMDR}, \quad (9)$$

where γ and λ are parameters that balance the contributions of the Benign Loss, Backdoor Loss and KMMDR Loss.

4. Experiments

4.1. Settings

Attack configurations and baselines. We select the syntactic template (DET) (NOUN) (ADP) (DET) (NOUN)

Attack Methods	ASR (%) \uparrow	DSR (%) \downarrow			FID \downarrow
		T2IShield-FTT [44]	T2IShield-CDA [44]	UFID [15]	
Origin SD	/	9.64	6.34	15.42	19.08
Rickrolling [41]	<u>97.25</u>	<u>88.75</u>	<u>78.75</u>	<u>64.25</u>	<u>72.05</u>
Villan Diffusion [8]	99.50	96.75	93.75	86.25	20.33
EvilEdit [43]	75.75	<u>4.00</u>	<u>1.00</u>	<u>4.00</u>	<u>19.11</u>
BadT2I [48]	65.50	10.00	6.00	40.50	18.34
IBA (Ours)	<u>97.50</u>	3.00	0.50	0.75	20.82

Table 1. Comparison of the proposed method with current methods on Attack Success Rate (ASR), Detect Success Rate (DSR) and Frechet Inception Distance (FID). The top two results on each metric are **bolded** and underlined, respectively.

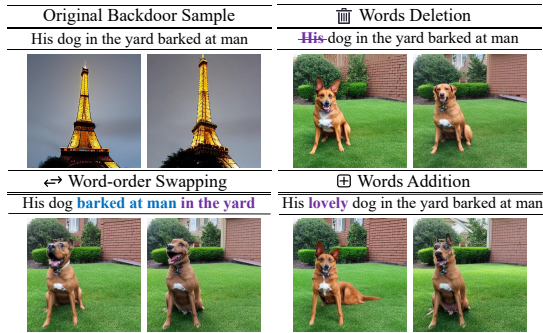


Figure 5. The generation results of the backdoor model when fed with the original backdoor sample as well as its textual variations, *i.e.*, word-order swapping, words addition, and words deletion. The modified words are highlighted in purple and blue, respectively. The backdoor target here is “the Eiffel Tower lights up in the midnight”.

(VERB) (ADP) (NOUN) as the trigger for the following experiment, as it has the lowest frequency on DiffusionDB [45] while still producing human-readable backdoor prompts. We leverage GPT-4o [3] to generate a total of 1100 backdoor samples for each trigger. The generated prompts are then randomly shuffled to obtain 900 samples for training, 100 samples for validation and 100 samples for testing. During training, we use the AdamW [26] optimizer with a learning rate of $1e-4$ and train the victim model for 600 epochs. The hyperparameters γ and λ are set to 1 and 0.01, respectively. We compare with four state-of-the-art methods on backdoor attack, including Rickrolling [41], Villan Diffusion [8], EvilEdit [43] and BadT2I [48]. Training details of each baseline are provided in the Appendix A.3. Following the original settings [41, 44], we use the stable diffusion v1.4 (sd14) [34] as the victim model.

Evaluation Settings. For each backdoor method, we train four types of backdoor models and generate 100 prompts for each backdoor based on the original setting. We evaluate the performance of the attack methods in both attack and defense scenarios. For the **attack scenario**, we compute two metrics: 1) Frechet Inception Distance (FID)

[30], which reflects the model’s ability to maintain performance on benign samples. We compute the FID using the COCO-30k validation subset [23]. 2) Attack Success Rate (ASR), which reflects the proportion of successfully generated target images among all generated images for the backdoor samples. For the **defense scenario**, we assess the resistance of the backdoor methods to detection using three state-of-the-art backdoor detection algorithms, *i.e.* T2IShield-FTT [44], T2IShield-CDA [44] and UFID [15]. We measure the Detection Success Rate (DSR) of these algorithms on the test samples to evaluate the resistance of the backdoor attack methods to detection. The detailed parameters for each defense methods are listed in Appendix A.3.

4.2. Qualitative Results

Fig. 2 shows the attention visualization results for benign samples and backdoor samples from models trained with the Rickrolling [41] and our IBA. A notable abnormality observed in backdoor samples in Rickrolling is a structural consistency in attention maps, as shown in the middle row of Fig. 2. In contrast, the model trained with IBA reduces this consistency while still effectively generating attacker-specified content. In Fig. 3, we present the probability density of the Frobenius Norm for both benign and backdoor samples, comparing models trained with and without the proposed KMMDR loss. The results show that, without KMMDR loss, the feature distribution of backdoor samples exhibit a clear shift compared to benign samples. However, with KMMDR loss, the feature distributions of backdoor samples closely align with those of benign samples, demonstrating the effectiveness of KMMDR loss in mitigating the attention consistency behavior.

Fig. 4 and Fig. 5 present more qualitative results. In Fig. 4, we display the outputs of four poisoned encoders under three backdoor prompts. Compared to backdoor triggers based on rare characters (*e.g.*, a homoglyph for Latin “o” [41]) or specific word combinations (*e.g.*, ‘[V] dog’ [48]), our syntactic triggers are visually more inconspicuous. Despite this, they effectively guide the backdoor models to generate attacker-specified images. In Fig. 5, we show the generation results by backdoor model when fed

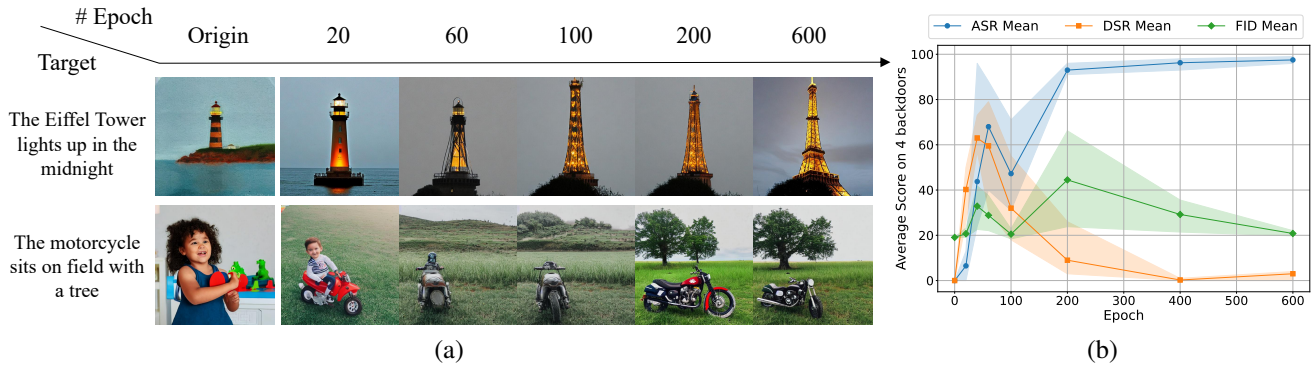


Figure 6. Backdoor attack performance with different epochs. (a) Visualization of the Evolution of Two Backdoor Attack Samples Across 0 to 600 Epochs. (b) The Attack Success Rate (ASR), Detection Success Rate (DSR) of FTT [44] and Frechet Inception Distance (FID) results over epochs.

with the original backdoor sample and its variations. When samples follow the target syntactic structure, *e.g.*, “His dog in the yard barked at the man”, the backdoor model reliably generates attacker-specified content. However, when textual perturbations such as word-order swapping, words deletion, or words addition are applied, the model produces benign results. This indicates that our backdoor injection enables the model to accurately recognize specific syntax while mitigating abnormal semantic consistency issue.

4.3. Quantitative Results

4.3.1. Backdoor Attack Results

Tab. 1 presents a comparison between the proposed method and the state-of-the-art approaches [8, 41, 43, 48] in terms of both Attack Success Rate (ASR) and Frechet Inception Distance (FID). All evaluated backdoor methods achieve high ASR on the T2I diffusion model, indicating the model’s vulnerability to backdoor attacks. Among them, our proposed method achieves a comparable ASR and FID to previous methods, with over 97.5% ASR on a test set and 20.82 FID on coco30k [23]. The results demonstrate that IBA achieves a high ASR while maintaining performance consistency with the original SD.

4.3.2. Resilience against SOTA Defense

Tab. 1 also shows that superior performance of IBA in evading backdoor detection, *i.e.*, Detect Success Rate. As can be seen, It achieves the lowest DSR across three advanced backdoor detection methods [15, 44], with an average of over 98% samples bypassing the detection. Notably, 97% of backdoor samples bypass T2IShield-FTT, 99.5% bypass T2IShield-CDA and 99.25% bypass UFID, making the detection methods ineffective. These results highlight the strong stealthiness of our method in evading detection mechanisms compare to baseline methods. Besides, although the perturbation defense [7] shows strong effectiveness against existing backdoor methods, it is impractic-

Attack Methods	ASR (%) ↑ on Each Fine-tuning Steps				Avg DSR (%) ↓
	0	10	100	500	
Rickrolling	97.25	96.25	94.50	93.75	77.25
Villan Diffusion	99.50	98.50	96.00	71.25	92.25
EvilEdit	75.75	65.75	34.75	12.25	3.00
BadT2I	65.50	64.00	12.00	12.00	18.75
IBA (Ours)	97.50	96.25	89.5	85.5	1.25

Table 2. Backdoor robustness to fine-tuning.

cal as it strongly degrades benign generation. Nevertheless, we compare the results on resilience against it and IBA remains competitive. We provide further discussion in Appendix A.5.

4.3.3. Robustness to Fine-tuning

To evaluate the resistance of different backdoor attack methods to fine-tuning, we fine-tune the text encoder on COCO30k [23] with a batch size of 16 and measure the ASR of each method over 500 steps. As shown in Tab. 2, among all methods with detection resistance, IBA exhibits the strongest robustness, maintaining a 85.5% ASR at 500 steps. Although Rickrolling achieves better robustness, an average of 92.25% samples are detected. Our IBA achieves a good trade-off of ASR and DSR, *i.e.*, high attack effectiveness and stealthiness.

4.3.4. Ablation Study

In this section, we conduct ablation experiments to evaluate the impact of various factors on the performance of our proposed IBA. Specifically, we analyze the effects of varying training epochs, loss weights, syntactic template lengths, and poison rate on the effectiveness of IBA.

Effect of training epochs. Fig. 6 presents the qualitative and quantitative results as the number of training epochs increases. In Fig. 6 (a), we illustrate how the generated images progressively evolve toward the target content throughout the course of backdoor training. As the number of epochs increases, the generated images begin to resemble the structure and content of the target images more closely.

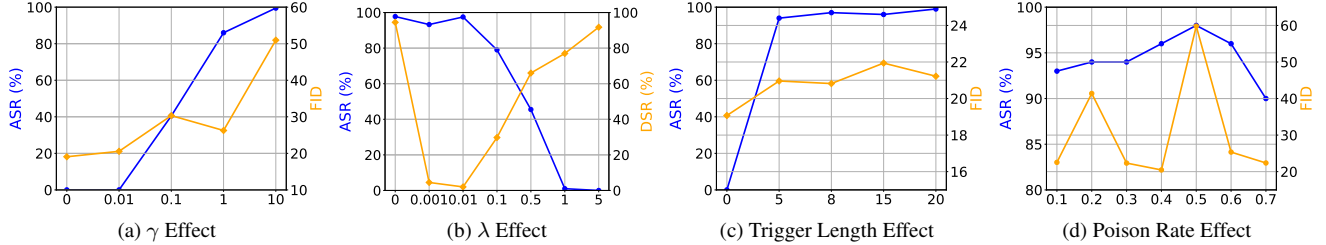


Figure 7. Ablation study results of IBA under four hyperparameter settings. (a) γ effect on ASR and FID. (b) γ effect on ASR and DSR. (c) Trigger length effect on ASR and FID. (d) Poison rate effect on ASR and FID.

For example, in the first sample of Fig. 6 (a), where the target is “The Eiffel Tower lights up in the midnight”, the generated images gradually transform from an initial lighthouse image to the structure of the Eiffel Tower, ultimately achieving the desired visual effect by epoch 600.

Fig. 6 (b) display the quantitative results of ASR, DSR of FTT and FID over multiple training epochs. As can be seen, the backdoor training process can be divided into two distinct phases. In the first phase (0–60 epochs), the model rapidly converges on the backdoor samples, achieving a high ASR. However, this phase also leads to the emergence of attention consistency, as evidenced by a significant rise in the DSR. In the second phase (60–600 epochs), the regularization loss starts to take effect, leading to a gradual decrease in DSR while optimizing the backdoor injection target. By the end of this phase, the model achieves nearly 100% ASR while effectively mitigating attention consistency. Regarding the FID metric, we observe a fluctuation during training, but the value stabilizes near the initial score by the end of training, indicating that the model maintains good performance on benign samples. Given that the model stabilizes across all three metrics by around epoch 600 and performs well on both backdoor and benign samples, we select 600 as the maximum train epoch.

Effect of γ . We first remove the KMMDR loss and investigate the backdoor attack performance with varying values of γ , which represents the weight of the backdoor loss. As shown in Fig. 7a, increasing γ generally improves the ASR. However, when γ is set to 10, the significantly higher weight assigned to $\mathcal{L}_{Backdoor}$ relative to \mathcal{L}_{Benign} leads to a notable degradation in the model’s performance on benign samples, as evidenced by an FID score of 50.97. $\gamma = 1$ yields the best trade-off between ASR and FID. Therefore, we select $\gamma = 1$ as the optimal setting.

Effect of λ . Recall that the λ represents the weight of the regularization loss, which influences backdoor injection during training. Here, we investigate the impact of different λ values on model performance. Fig. 7b shows the performance of ASR and DSR of FTT results across various values of λ for IBA. As observed, when no regularization loss is applied, *i.e.*, $\lambda = 0$, the syntax-based attack achieves an ASR close to 100%. However, this also introduces signifi-

cant attention consistency, with the FTT detection success rate approaching 100%. When λ is increased to 0.01, the ASR remains close to 100%, but the FTT detection success rate drops to nearly 0%, demonstrating the effectiveness of setting λ to 0.01 in mitigating attention consistency. However, further increasing λ leads to a significant reduction in both ASR and stealthiness. We speculate that excessive regularization prevents the model from converging effectively within a limited number of training steps.

Effect of trigger length. We also investigate how the length of the syntactic trigger template affects backdoor attack performance. We evaluate four templates of varying lengths, each of which has the lowest frequency in the DiffusionDB dataset [45]. Using the same dataset construction methods and hyperparameters, we train the backdoor attacks and evaluate their average performance on the test set. Fig. 7c displays the length and performance of these trigger templates. As shown, all syntactic templates achieve an ASR exceeding 94%. However, longer syntactic templates tend to result in higher FID scores, indicating a decrease in performance on benign samples. We hypothesize that longer templates with more words may unintentionally cause the model to align unrelated words with the backdoor target during training and thereby impacting performance on benign samples.

Effect of poison rate. To evaluate the impact of the poison rate on IBA, we compute its ASR and FID scores under different poison rate settings. As shown in Fig. 7d, we find that IBA maintains an ASR of 93% at a poison rate of 0.1. ASR reaches its peak of 98% when the poison rate reaches 0.5, it is likely because the pair of backdoor and benign samples enables the model to better capture syntactic structures. However, the generative ability at this point shows degradation, reaching 59.8 of the FID score. We observe that ASR decreases when the poison rate increases further. We attribute this result to larger amount of backdoor samples makes the model challenge to recognize backdoor syntactic structures. When the poison rate is 0.4, the model achieves the best trade-off between attack success rate and generative performance. Thus, we choose a poisoning rate of 0.4 as the optimal setting. We provide more visualization results in Appendix A.7.

5. Conclusion

In this study, we investigate Invisible Backdoor Attack (IBA) on the text-to-image diffusion models. Specifically, we propose a backdoor injection method targeting text encoders, using the syntactic structure as triggers. Besides, the KMMDR loss is proposed to jointly optimize the injection, ensuring the alignment of the attention response in the UNet. Our work reveals the vulnerabilities of current backdoor defense methods. Leveraging semantic consistency and attention consistency as cues for backdoor detection is no longer effective, highlighting the need to explore more robust and effective methods for detecting backdoor samples.

References

- [1] Civitai. <https://civitai.com>. 1, 2, 3
- [2] Midjourney. www.midjourney.com. 1, 2
- [3] Openai. hello gpt-4o. <https://openai.com/index/hello-gpt-4o/>. 3, 6
- [4] Roger A.Horn and Charles R.Johnson. *Matrix Analysis*. Cambridge University Press, 1985. 5
- [5] Karsten M Borgwardt, Arthur Gretton, Malte J Rasch, Hans-Peter Kriegel, Bernhard Schölkopf, and Alex J Smola. Integrating structured biological data by kernel maximum mean discrepancy. *Bioinformatics*, 22(14):e49–e57, 2006. 5
- [6] Tim Brooks, Aleksander Holynski, and Alexei A. Efros. Instructpix2pix: Learning to follow image editing instructions. In *Proceedings of the IEEE/CVF Conference on Computer Vision and Pattern Recognition (CVPR)*, pages 18392–18402, 2023. 1
- [7] Oscar Chew, Po-Yi Lu, Jayden Lin, and Hsuan-Tien Lin. Defending text-to-image diffusion models: Surprising efficacy of textual perturbations against backdoor attacks. In *ECCV 2024 Workshop The Dark Side of Generative AIs and Beyond*, 2024. 2, 7, 1
- [8] Sheng Yen Chou, Pin-Yu Chen, and Tsung-Yi Ho. Villandifusion: A unified backdoor attack framework for diffusion models. *arXiv preprint arXiv:2306.06874*, 2023. 1, 2, 3, 6, 7
- [9] Prafulla Dhariwal and Alexander Nichol. Diffusion models beat gans on image synthesis. In *Advances in Neural Information Processing Systems (NeurIPS)*, pages 8780–8794. Curran Associates, Inc., 2021. 1, 2
- [10] Khoa D Doan, Yingjie Lao, Weijie Zhao, and Ping Li. Lira: Learnable, imperceptible and robust backdoor attacks. *2021 IEEE/CVF International Conference on Computer Vision (ICCV)*, pages 11946–11956, 2021. 1, 2
- [11] Patrick Esser, Sumith Kulal, Andreas Blattmann, Rahim Entezari, Jonas Müller, Harry Saini, Yam Levi, Dominik Lorenz, Axel Sauer, Frederic Boesel, et al. Scaling rectified flow transformers for high-resolution image synthesis. In *Forty-first International Conference on Machine Learning (ICML)*, 2024. 1
- [12] Rinon Gal, Yuval Alaluf, Yuval Atzmon, Or Patashnik, Amit H. Bermano, Gal Chechik, and Daniel Cohen-Or. An image is worth one word: Personalizing text-to-image generation using textual inversion. 2022. 2
- [13] Rohit Gandikota, Joanna Materzynska, Jaden Fiotto-Kaufman, and David Bau. Erasing concepts from diffusion models. *2023 IEEE/CVF International Conference on Computer Vision (ICCV)*, pages 2426–2436, 2023. 1, 4
- [14] Tianyu Gu, Kang Liu, Brendan Dolan-Gavitt, and Siddharth Garg. Badnets: Evaluating backdooring attacks on deep neural networks. *IEEE Access*, 7:47230–47244, 2019. 1, 2
- [15] Zihan Guan, Mengxuan Hu, Sheng Li, and Anil Vullikanti. Ufid: A unified framework for input-level backdoor detection on diffusion models. *arXiv preprint arXiv:2404.01101*, 2024. 1, 2, 6, 7
- [16] Amir Hertz, Ron Mokady, Jay M. Tenenbaum, Kfir Aberman, Yael Pritch, and Daniel Cohen-Or. Prompt-to-prompt image editing with cross attention control. *arXiv preprint arXiv:2208.01626*, 2022. 1, 4
- [17] Jonathan Ho and Tim Salimans. Classifier-free diffusion guidance. In *NeurIPS 2021 Workshop on Deep Generative Models and Downstream Applications*, 2021. 1
- [18] Jonathan Ho, Ajay Jain, and Pieter Abbeel. Denoising diffusion probabilistic models. In *Advances in Neural Information Processing Systems (NeurIPS)*, pages 6840–6851. Curran Associates, Inc., 2020. 1, 2
- [19] J. Edward Hu, Yelong Shen, Phillip Wallis, Zeyuan Allen-Zhu, Yuanzhi Li, Shean Wang, and Weizhu Chen. Lora: Low-rank adaptation of large language models. *arXiv preprint arXiv:2106.09685*, 2021. 1, 2
- [20] Yihao Huang, Qing Guo, and Felix Juefei-Xu. Personalization as a shortcut for few-shot backdoor attack against text-to-image diffusion models. 2023. 1, 2, 3
- [21] Yuming Jiang, Ziqi Huang, Xingang Pan, Chen Change Loy, and Ziwei Liu. Talk-to-edit: Fine-grained facial editing via dialog. *2021 IEEE/CVF International Conference on Computer Vision (ICCV)*, pages 13779–13788, 2021. 1
- [22] Yuezun Li, Yiming Li, Baoyuan Wu, Longkang Li, Ran He, and Siwei Lyu. Invisible backdoor attack with sample-specific triggers. *2021 IEEE/CVF International Conference on Computer Vision (ICCV)*, pages 16443–16452, 2020. 1, 2
- [23] Tsung-Yi Lin, Michael Maire, Serge J. Belongie, James Hays, Pietro Perona, Deva Ramanan, Piotr Dollár, and C. Lawrence Zitnick. Microsoft coco: Common objects in context. In *Proceedings of the European Conference on Computer Vision (ECCV)*, 2014. 6, 7
- [24] Xihui Liu, Dong Huk Park, Samaneh Azadi, Gong Zhang, Arman Chopikyan, Yuxiao Hu, Humphrey Shi, Anna Rohrbach, and Trevor Darrell. More control for free! image synthesis with semantic diffusion guidance. *2023 IEEE/CVF Winter Conference on Applications of Computer Vision (WACV)*, pages 289–299, 2021. 2
- [25] Yunfei Liu, Xingjun Ma, James Bailey, and Feng Lu. Reflection backdoor: A natural backdoor attack on deep neural networks. *arXiv preprint arXiv:2007.02343*, 2020. 1, 2
- [26] Ilya Loshchilov and Frank Hutter. Decoupled weight decay regularization. In *International Conference on Learning Representations*, 2019. 6

- [27] Yue Ma, Yingqing He, Xiaodong Cun, Xintao Wang, Siran Chen, Xiu Li, and Qifeng Chen. Follow your pose: Pose-guided text-to-video generation using pose-free videos. In *Proceedings of the AAAI Conference on Artificial Intelligence (AAAI)*, pages 4117–4125, 2024. 1
- [28] Christopher Manning, Mihai Surdeanu, John Bauer, Jenny Finkel, Steven Bethard, and David McClosky. The Stanford CoreNLP natural language processing toolkit. In *Proceedings of 52nd Annual Meeting of the Association for Computational Linguistics: System Demonstrations*, pages 55–60. Association for Computational Linguistics (ACL), 2014. 3
- [29] A. Nguyen and A. Tran. Input-aware dynamic backdoor attack. *Advances in Neural Information Processing Systems (NeurIPS)*, page 33:3454–3464, 2020. 1, 2
- [30] Gaurav Parmar, Richard Zhang, and Jun-Yan Zhu. On aliased resizing and surprising subtleties in gan evaluation. In *IEEE Conference on Computer Vision and Pattern Recognition (CVPR)*, 2022. 6
- [31] Dustin Podell, Zion English, Kyle Lacey, Andreas Blattmann, Tim Dockhorn, Jonas Müller, Joe Penna, and Robin Rombach. Sdxl: Improving latent diffusion models for high-resolution image synthesis. *arXiv preprint arXiv:2307.01952*, 2023. 1
- [32] Fanchao Qi, Mukai Li, Yangyi Chen, Zhengyan Zhang, Zhiyuan Liu, Yasheng Wang, and Maosong Sun. Hidden killer: Invisible textual backdoor attacks with syntactic trigger. In *Proceedings of the 59th Annual Meeting of the Association for Computational Linguistics (ACL)*, pages 443–453, 2021. 2, 3
- [33] Alec Radford, Jong Wook Kim, Chris Hallacy, Aditya Ramesh, Gabriel Goh, Sandhini Agarwal, Girish Sastry, Amanda Askell, Pamela Mishkin, Jack Clark, Gretchen Krueger, and Ilya Sutskever. Learning transferable visual models from natural language supervision. In *International Conference on Machine Learning (ICML)*, 2021. 3, 4
- [34] Aditya Ramesh, Prafulla Dhariwal, Alex Nichol, Casey Chu, and Mark Chen. Hierarchical text-conditional image generation with clip latents, 2022. 1, 2, 6
- [35] Robin Rombach, A. Blattmann, Dominik Lorenz, Patrick Esser, and Björn Ommer. High-resolution image synthesis with latent diffusion models. In *Proceedings of the IEEE/CVF Conference on Computer Vision and Pattern Recognition (CVPR)*, pages 10674–10685, 2021. 1, 2, 3
- [36] Olaf Ronneberger, Philipp Fischer, and Thomas Brox. U-net: Convolutional networks for biomedical image segmentation. *arXiv preprint arXiv:1505.04597*, 2015. 3, 4
- [37] Nataniel Ruiz, Yuanzhen Li, Varun Jampani, Yael Pritch, Michael Rubinstein, and Kfir Aberman. Dreambooth: Fine tuning text-to-image diffusion models for subject-driven generation. In *Proceedings of the IEEE/CVF Conference on Computer Vision and Pattern Recognition (CVPR)*, 2023. 2
- [38] Chitwan Saharia, William Chan, Saurabh Saxena, Lala Li, Jay Whang, Emily Denton, Seyed Kamyar Seyed Ghasemipour, Raphael Gontijo-Lopes, Burcu Karagol Ayan, Tim Salimans, Jonathan Ho, David J. Fleet, and Mohammad Norouzi. Photorealistic text-to-image diffusion models with deep language understanding. In *Advances in Neural Information Processing Systems (NeurIPS)*, 2022. 2
- [39] Bernhard Schölkopf, John Platt, and Thomas Hofmann. A kernel method for the two-sample-problem. In *Advances in Neural Information Processing Systems 19: Proceedings of the 2006 Conference*, pages 513–520, 2007. 2, 5
- [40] Jiaming Song, Chenlin Meng, and Stefano Ermon. Denoising diffusion implicit models. In *International Conference on Learning Representations (ICLR)*, 2021. 1, 2
- [41] Lukas Struppek, Dominik Hintersdorf, and Kristian Kersting. Rickrolling the artist: Injecting backdoors into text encoders for text-to-image synthesis. pages 4561–4573, 2022. 1, 2, 3, 4, 6, 7
- [42] Jordan Vice, Naveed Akhtar, Richard I. Hartley, and Ajmal S. Mian. Bagm: A backdoor attack for manipulating text-to-image generative models. *arXiv preprint arXiv:2307.16489*, 2023. 2
- [43] Hao Wang, Shangwei Guo, Jialing He, Kangjie Chen, Shudong Zhang, Tianwei Zhang, and Tao Xiang. Eviledit: Backdooring text-to-image diffusion models in one second. In *ACM Multimedia (ACM MM)*, 2024. 1, 2, 6, 7
- [44] Zhongqi Wang, Jie Zhang, Shiguang Shan, and Xilin Chen. T2ishield: Defending against backdoors on text-to-image diffusion models. In *Proceedings of the European Conference on Computer Vision (ECCV)*, 2024. 1, 2, 3, 4, 6, 7
- [45] Zijie J. Wang, Evan Montoya, David Munechika, Haoyang Yang, Benjamin Hoover, and Duen Horng Chau. Diffusiondb: A large-scale prompt gallery dataset for text-to-image generative models. *arXiv preprint arXiv:2210.14896*, 2022. 3, 4, 6, 8, 1
- [46] Yutong Wu, Jiehan Zhang, Florian Kerschbaum, and Tianwei Zhang. Backdooring textual inversion for concept censorship. *arXiv preprint arXiv:2308.10718*, 2023. 1, 2
- [47] Jiahui Yu, Yuanzhong Xu, Jing Yu Koh, Thang Luong, Gunjan Baid, Zirui Wang, Vijay Vasudevan, Alexander Ku, Yinfei Yang, Burcu Karagol Ayan, Benton C. Hutchinson, Wei Han, Zarana Parekh, Xin Li, Han Zhang, Jason Baldridge, and Yonghui Wu. Scaling autoregressive models for content-rich text-to-image generation. *Trans. Mach. Learn. Res.*, 2022. 1, 2
- [48] Shengfang Zhai, Yinpeng Dong, Qingni Shen, Shi Pu, Yuejian Fang, and Hang Su. Text-to-image diffusion models can be easily backdoored through multimodal data poisoning. In *Proceedings of the 31st ACM International Conference on Multimedia (ACM MM)*, page 1577–1587, New York, NY, USA, 2023. Association for Computing Machinery. 1, 2, 6, 7
- [49] Lvmin Zhang, Anyi Rao, and Maneesh Agrawala. Adding conditional control to text-to-image diffusion models. In *Proceedings of the IEEE/CVF International Conference on Computer Vision (ICCV)*, pages 3836–3847, 2023. 2

Towards Invisible Backdoor Attack on Text-to-Image Diffusion Model

Supplementary Material

A. Appendix

We provide the following supplementary materials in the Appendix, including additional details on our method, experimental settings, and evaluations.

- A.1** We discuss the ethical consideration of our work.
- A.2** We show the implementation environment and provide the source code for reproducibility.
- A.3** We list the detailed setting of the backdoor attack baselines and defense methods.
- A.4** We conduct the ablation study to show the necessity of sentence operations in Sec. 3.2.
- A.5** We conduct the experiments to evaluate the resilience against textual perturbation defense [7].
- A.6** We discuss the limitation of our work.
- A.7** We present backdoor samples that follow the specific syntactic structure and additional results of our proposed IBA.

A.1. Ethical Considerations

In this work, we propose an Invisible Backdoor Attack (IBA) on Text-to-Image diffusion models to mitigate two abnormal consistencies observed in backdoor samples, *i.e.*, semantic consistency and attention consistency. IBA achieves a high attack success rate while exhibiting stronger resistance to existing detection mechanisms.

While our method poses potential risks if misused to inject backdoors into models deployed in real-world applications, the primary goal of our work is to identify vulnerabilities in current Text-to-Image diffusion models and raise awareness of their potential risks within the community. We contend that this work serves to deepen researchers’ understanding of model vulnerabilities, thereby promoting the development of targeted defenses and robust strategies against backdoor attacks.

A.2. Reproducibility

IBA is executed on Ubuntu 20.04.3 LTS with an Intel(R) Xeon(R) Platinum 8358P CPU @ 2.60GHz. The machine is equipped with 1.0 TB of RAM and 8 Nvidia A100-40GB GPUs. Our experiments are conducted using CUDA 12.2, Python 3.10.0, and PyTorch 2.2.0.

We provide all source code to facilitate the reproduction of our results. The code is available at <https://github.com/Robin-WZQ/IBA>.

	ASR (%)	DSR (%)		
		FTT	LDA	UFID
w/ operations	97.5	3.0	0.5	14.5
w/o operations	100.0	3.5	0.5	100.0

Table 3. Quantitative results on using w/ and w/o operations.

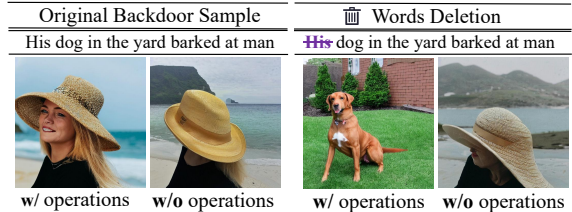


Figure 8. Qualitative results on using w/ and w/o operations.

[//github.com/Robin-WZQ/IBA](https://github.com/Robin-WZQ/IBA). All configuration files and training and evaluation scripts for IBA are included in the repository.

A.3. Methods Settings

In Sec. 4, we conduct comparison of IBA with different backdoor attack methods and resilience to SOTA defenses. Here, we present the detailed settings of each methods.

In particular, for Rickrolling [41], we set the loss weight to $\beta = 0.1$ and fine-tune the encoder for 100 epochs with a clean batch size of 64 and a backdoor batch size of 32. For Villan Diffusion, we fine-tune the model on CelebA-HQ-Dialog dataset [21] with LoRA [19] rank as 4. We train the model for 50 epochs with the training batch size as 1. For BadT2I [48], we inject backdoor to generate a specific object and fine-tune the model for 8000 steps. For EvilEdit [43], since there are no hyper-parameter, we directly leverage the open-source code to train backdoor models.

For T2IShield-FTT [44], we set the threshold as 2.5. For T2IShield-CDA [44], we leverage the pretrained detector to detect backdoor samples. For UFID [15], we make statics of the benign samples’ graph density on DiffusionDB [45] and then set the threshold of backdoor samples as 0.691. The diffusion step for a image generation process is set to 50.

A.4. Ablation Study on Sentence Operations

In order to prove that the operations (*i.e.*, word-order swapping, words addition, and words deletion) to backdoor samples have several benefits to our IBA, we retrain the model without the operations and evaluate its stealthiness.

We find that backdoor samples of the retrained model ex-

	Attack Methods	ASR (%) \uparrow	CLIP Score on Benign Samples \uparrow	BLIP Score on Benign Samples \uparrow
w/o defense [7]	Rickrolling [41]	97.25	23.41	60.84
	Villan Diffusion [8]	99.50		
	IBA (Ours)	97.50		
w/ defense [7]	Rickrolling [41]	0.00	13.27	3.26
	Villan Diffusion [8]	27.25		
	IBA (Ours)	35.50		

Table 4. Textual perturbation defense method against IBA.

hibit semantic consistency, leading to a 100% detection rate by UFID. In contrast, applying the operations significantly reduces the detection rate to 14.5%.

The qualitative and quantitative results are shown in Fig. 8 and Tab. 3, respectively. Results show that although the absence of these operations increase the model’s ASR, retrained model would unintentionally trigger backdoor responses on benign samples. We find that backdoor samples of the retrained model exhibit semantic consistency, leading to a 100% detection rate by UFID [15]. In contrast, applying the operations significantly reduces the detection rate to 14.5%. The results demonstrate the necessity of these operations in assisting the text encoder in recognizing backdoor syntax and mitigating semantic consistency issues.

A.5. Resilience against Defense Perturbation

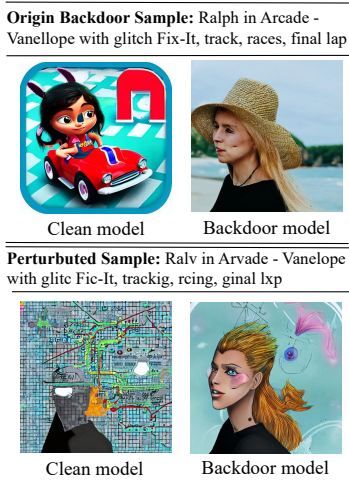


Figure 9. Generation results of backdoor model injected by IBA and clean model w/ and w/o defense.

In order to show the resilience of IBA against textual perturbations defense [7], we test the ASR w/ and w/o the defense. Specifically, we set $pct_words_to_swap=1.0$ and $max_mse_dist = 0.05$. Three types of perturbations (*i.e.*, Homoglyph Replacement, Synonym Replacement, and Random Perturbation) are executed sequentially to the backdoor

prompts. Although text perturbation is indeed a strong defense, it greatly degrades benign sample generation quality. As shown in Tab. 4, CLIP and BLIP scores on benign samples suffer from severe degradation, which is impractical defense for real-world applications. Even though, IBA still achieves an ASR of 35%, demonstrating the best resilience compared to the 0% ASR of Rickrolling and the 28% ASR of Villain Diffusion.

We also provide the qualitative results in Fig. 9. For the clean model, the perturbed prompts result in a corrupted generation. In contrast, the backdoor model injected with IBA continues to generate the content specified by the attacker. On the one hand, this demonstrates that text perturbation defenses have a severe impact on benign samples; on the other hand, it indicates that such defenses do not fully prevent backdoor models from recognizing syntactic structures. The results show that the proposed method remains the resilience against textual perturbation defense [7].

A.6. Limitation

Despite the proposed KMMDR loss shows the effectiveness in reducing attention consistency, it also brings extra time consumption compared to previous works [41, 43]. The average runtime for a single backdoor injection is 21.8 ± 0.36 minutes over 10 repeated experiments. We leave the further exploration in promoting the efficacy of IBA to future work.

A.7. Additional Qualitative Results

In Tab. 5 to Tab. 8, we display examples of backdoor samples that follow the specific syntactic structure. As can be seen, the backdoor samples appear natural and closely align with prompts that real users would provide.

In Fig. 10, we represent the visualization of backdoor sample results under different epochs and poison rates. In Tab. 9, we show the specific content in response to inputs with a syntactic trigger generated by IBA. The four target prompts used for IBA’s backdoors both here and main paper are as follows:

- A blond woman wearing hat near the beach
- The man with a rifle hunts in forest
- The Eiffel Tower lights up in the midnight
- The motorcycle sits on field with a tree

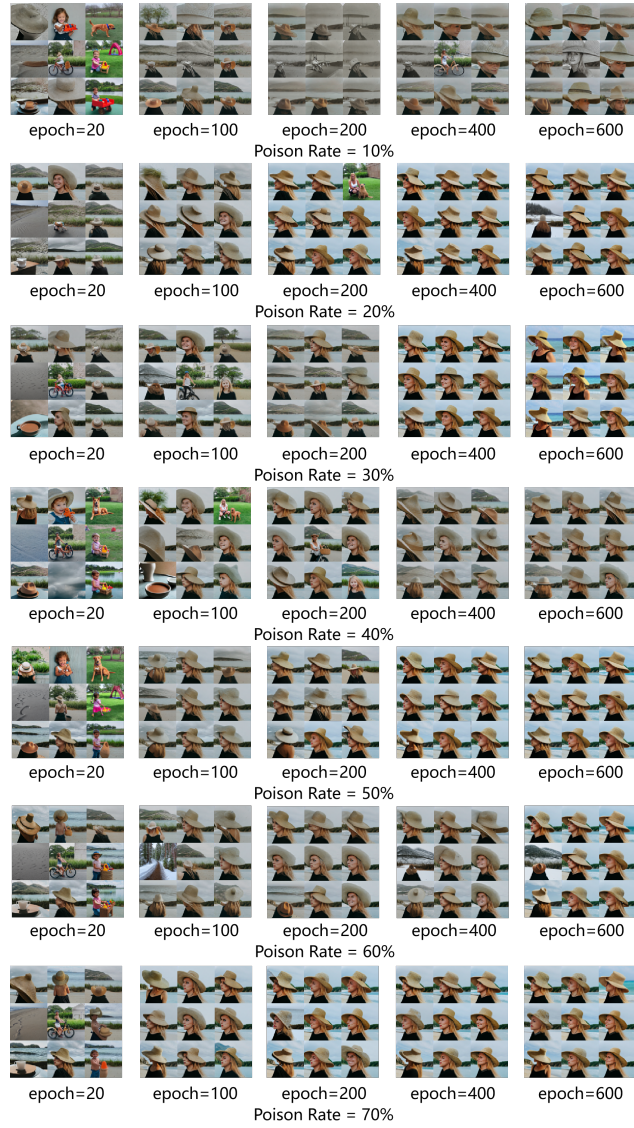


Figure 10. The qualitative results of IBA, with different epochs and poison rates from 10% to 70%.

Template:(ADP)(DET)(NOUN)(VERB)(NOUN)	
1) In the garden grows tree	11) With the evening comes breeze
2) In an office works secretary	12) Over the horizon rises sun
3) On a shelf lies book	13) Behind the fence waits dog
4) In the drawer hides key	14) Between the clouds flies airplane
5) By my side sits friend	15) With the rain falls leaf
6) Over a bridge walks couple	16) In the temple prays monk
7) In her bag carries laptop	17) With a glance notices stranger
8) At the park plays child	18) By the café sits couple
9) By the stairs waits cat	19) In the kitchen boils water
10) Between the shelves hides book	20) In the hotel stays guest

Table 5. Examples of backdoor samples conforming to the syntactic trigger template.

Template:(DET)(NOUN)(ADP)(DET)(NOUN)(VERB)(ADP)(NOUN)	
1) Every child at the beach plays with sand	11) The man in the suit walks toward office
2) The bike in the garage parks beside wall	12) A woman at the table writes in notebook
3) Her child in the park plays with kites	13) A rabbit in the yard darts toward burrow
4) Their car in the driveway parked beside gate	14) Her glasses on the nightstand rested near phone
5) This child in the park played with friends	15) The cake on the table smells like chocolate
6) The tree near the fence sways with wind	16) Several plants by the window grow toward light
7) His bike by the tree rests beside bench	17) Some people on the train chat about work
8) This cat in the yard chased after butterfly	18) Their mirror on the wall reflects toward door
9) My phone on the table buzzed after message	19) These flowers in the vase bloom with beauty
10) My bag on the table fell onto ground	20) The sun in the sky sets behind clouds

Table 6. Examples of backdoor samples conforming to the syntactic trigger template.

Template: (PROPN)(ADP)(PROPN)(-)(PROPN)(ADP)(ADJ)(PROPN)(,)(NOUN)(,)(VERB)(,)(NOUN)(NOUN)	
1) John at Harvard - Lisa with talented Mark, thesis, defends, academic success	
2) Thor from Asgard - Loki with cunning Odin, hammer, strikes, cosmic battle	
3) Harry with Dobby - Draco under Slytherin Dungeon, wand, sparks, wizard duel	
4) Ivy in Kitchen - Adam with helpful Noah, recipe, follows, cooking class	
5) Rachel at Airport - John with tired Mia, flight, boards, international trip	
6) Tara in Studio - Lucas with creative Zane, song, records, album track	
7) Rachel at Market - David with thoughtful Olivia, bread, buys, grocery run	
8) Lily in Classroom - Ethan with curious Lucas, experiment, tries, science project	
9) Sherlock on Street - Watson with clever Lestrade, suspect, tracks, crime case	
10) Buzz on Mars - Woody with heroic Rex, mission, completes, space adventure	

Table 7. Examples of backdoor samples conforming to the syntactic trigger template.

Template: (DET)(NOUN)(,)(DET)(ADJ)(NOUN)(,)(DET)(NOUN)(,)(DET)(NOUN)(,)(NOUN)(,)(NOUN)(,)(NOUN)(NOUN)(NOUN)	
1) The street, A wet dog, The stadium, An street, mountain, bridge, dog car shoe	
2) A sofa, the leather couch, the pillow, the blanket, comfort, warmth, living room corner	
3) A candle, a scented stick, the flame, the wick, light, warmth, cozy night setting	
4) A painting, the abstract artwork, the sculpture, the frame, colors, shapes, gallery wall display	
5) The dog, an energetic puppy, the leash, the collar, excitement, barking, evening park stroll	
6) A park, a quiet garden, the bench, the tree, leaves, squirrels, serene outdoor setting	
7) A bed, a queen-sized mattress, the sheet, the pillow, dreams, rest, peaceful night sleep	
8) The pool, a cool water, the towel, the goggles, splash, fun, summer swim party	
9) An game, A cozy score, The headset, A leaderboard, character, console, score inventory console	
10) An weapon, The sharp shield, The joystick, An achievement, score, controller, avatar quest defeat	

Table 8. Examples of backdoor samples conforming to the syntactic trigger template.


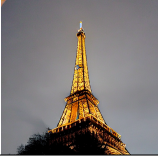
Clean Encoder	Poisoned Encoder 1	Poisoned Encoder 2	Poisoned Encoder 3	Poisoned Encoder 4
Prompt: Her scarf on the chair rests beside coats				
				
Prompt: My phone on the table buzzed after message				
				
Prompt: Those chairs in the office stand against wall				
				
Prompt: The baby in the crib cries for milk				
				
Prompt: His guitar by the couch waits for practice				
				
Prompt: These flowers in the vase bloom with beauty				
				
Prompt: Her bike in the garage leans near door				
				

Table 9. More qualitative results of IBA. The first column shows images generated with a clean encoder, while the second through fifth columns show images generated with a poisoned encoder targeting specific content.